

The bulk alloy microstructure and mechanical properties of Sn–1Ag–0.5Cu–xAl solders ($x = 0, 0.1$ and 0.2 wt. %)

Dhafer Abdul-Ameer Shnawah · Mohd Faizul Mohd Sabri ·
Irfan Anjum Badruddin · Suhana Binti Mohd Said ·
Fa Xing Che

Received: 5 December 2011 / Accepted: 12 March 2012 / Published online: 28 March 2012
© Springer Science+Business Media, LLC 2012

Abstract This work investigates the effects of 0.1 and 0.2 wt. % Al additions on bulk alloy microstructure and tensile properties as well as on the thermal behavior of Sn–1Ag–0.5Cu (SAC105) lead-free solder alloy. The addition of Al reduces the amount of Ag_3Sn intermetallic compound (IMC) particles and leads to the formation of larger Al–Ag IMC particles. Moreover, the addition of Al suppresses the formation of Cu_6Sn_5 IMC particles and leads to the formation of larger Al–Cu IMC particles. The Al added solders show a microstructure with large primary β -Sn grains. The tensile tests show that the 0.1 wt. % Al addition reduces the elastic modulus, yield strength and ultimate tensile strength (UTS). However, the 0.2 wt. % Al addition brings the yield strength up to SAC105 level and the UTS up to level slightly higher than that of SAC105, while its effect on reducing the elastic modulus becomes less dependent compared with the 0.1 wt. % Al addition. Moreover, both 0.1 and 0.2 wt. % Al additions deteriorate the total elongation. The two additions of Al slightly increase the solidus and liquids temperatures, while slightly reduce the pasty range, hence allowing the use of the Al-containing Sn–1Ag–0.5Cu alloys, to be consistent with the conditions of usage for conventional Sn–Ag–Cu solder alloys.

1 Introduction

Traditionally, Sn–Pb solder alloy has been the main soldering material for modern electronic packaging because of its superior performance and low cost. The presence of Pb in Sn–Pb solder alloys, mostly in the composition of eutectic 63Sn–37Pb, makes the solder superior in terms of its thermal and mechanical characteristics for microelectronic assembly and reliability [1]. However, the inherent toxicity of Pb has raised serious environmental and public health concerns [2–4]. The high Ag-content Sn–Ag–Cu alloys such as Sn–4 wt. %Ag–0.5 wt. %Cu (SAC405) or Sn–3 wt. %Ag–0.5 wt. %Cu (SAC305) have been considered promising replacements for the Sn–Pb solder alloy for microelectronics applications based on low available melting temperature, near eutectic composition and good cyclic fatigue properties [5]. However, due to the rigidity of the high Ag-content SAC alloys compared with the Sn–Pb solder alloy, more drop and high impact failures have been observed for these replacement alloys in portable electronic products such as personal data assistants (PDA), cellular phones, and notebook computers which all require good drop impact reliability [2, 6–11]. The root cause of the poor drop impact reliability of the high Ag-content SAC alloys lies in the bulk alloy properties. These high Ag-content SAC alloys have a relatively high elastic modulus and yield strength and small elongation, which result in a stiff bulk solder joint. This stiff bulk solder more readily transfer stress to the solder/substrate interface under conditions of drop. The intermetallic compound (IMC) layers formed at solder/substrate interface are of low ductility and exhibit brittle failure [12–14]. Moreover, the price competitiveness of the high Ag-content SAC alloys is a weak point due to the high cost of Ag [15]. Thus, there is a demand for a soft, highly compliant and relatively

D. A.-A. Shnawah (✉) · M. F. M. Sabri · I. A. Badruddin
Department of Mechanical Engineering, University of Malaya,
50603 Kuala Lumpur, Malaysia
e-mail: dhafer_eng@yahoo.com

S. B. M. Said
Department of Electrical Engineering, University of Malaya,
50603 Kuala Lumpur, Malaysia

F. X. Che
Institute of Microelectronics, A*STAR (Agency for Science,
Technology and Research), 11 Science Park Road, Singapore
Science Park II, Singapore 117685, Singapore

inexpensive alloy as a replacement for the high Ag-content SAC alloys for drop and high impact applications. Low Ag-content SAC alloys such as Sn–1 wt. %Ag–0.5 wt. %Cu (SAC105) have been considered a solution for resolving both issues [16]. Reducing the Ag content of the SAC alloy has been shown to reduce the elastic modulus and yield strength and increase the elongation of the bulk solder. This, in turn increases the elastic compliance and the plastic energy dissipation ability of the bulk solder, which are key factors to enhancing the drop resistance [17]. To further enhance the drop resistance, a family of low Ag-content SAC alloys doped with minor alloying additions such as Ni, Mn, Ce, Ti, In, Cr and Al have been investigated [13, 18–22]. Al is a low-cost element, and the use of Al is regarded as environmentally friendly, as Al is a non-hazardous material. Moreover, Al can change the intermetallic phases formed at the interface. However, a literature search revealed that few studies have been reported so far on the effect of Al addition on Sn–Ag–Cu solder joint quality. Generally, the formation and growth rate of the interface intermetallic compound (IMC) layer, the compliance of the bulk solder and the solder's wetting properties are the most influential factors in drop impact tests. Gain et al. [23] reported that the additions of 1 and 3 wt. % Al nanoparticles to the eutectic Sn–3.5Ag–0.5Cu solder on a Ni/Au surface finish improved the shear strength of the solder joints after multi-reflow and the following solid-state aging. The improvement in shear strength was attributed to a second phase dispersion strengthening mechanism through the formation of fine Sn–Ag–Al intermetallic compound particles and a controlled fine microstructure. Moreover, the effect of 1.5 wt. % Al addition on the interfacial reaction between the eutectic Sn–3.5Ag solder and Cu or Ni(P)/Au substrates was investigated by Jee et al. [24]. These authors reported that the addition of 1.5 wt. % Al to the Sn–3.5Ag solder on Cu suppressed the formation of Cu_6Sn_5 and Cu_3Sn IMC layers and led to the formation of a very thin CuAl_2 IMC layer. The CuAl_2 IMC layer acts as a diffusion barrier to the reaction between Cu and Sn, with the result that it hardly grows during aging. Moreover, the addition of 1.5 wt. % Al to the Sn–3.5Ag solder on Ni(P)/Au introduces a very thin, mixed IMC layer (Ni_3Sn_4 and Al_3Ni_2) and completely suppresses the formation of the Ni_3P layer. However, Kotadia and co-workers [25] demonstrated that the addition of Al in the range of 0.5 wt. % to 2 wt. % to a limited volume eutectic Sn–3.5Ag solder on Cu or Ni(P)/Au substrates does not change the formation and growth rate of the Cu–Sn and Ni–Sn IMC layers after reflow and the following solid-state aging. The effect of Al addition on SAC105 solder joint in terms of wettability and drop impact reliability was investigated by Lee et al. [22]. They found that Al addition in the range of 0.005–0.02 wt. % to SAC105 solder on Cu–OSP substrate

leads to a greater wetting force and shorter wetting time than the SAC105 solder, but Al addition over 0.1 wt. % resulted in poor wetting properties due to an increase in surface oxide. In general, Al metal easily forms Al oxide in the Sn–Ag–Cu solder system because the activation energy of Al oxide is lower than that of Sn oxide. Moreover, the additions of 0.005–0.02 wt. % Al to the SAC105 solder on an OSP surface finish improved its drop impact performance beyond the SAC105 solder. The extrinsic toughening of the bulk solder is possibly a very effective way to improve the drop impact reliability of solder joints, since its applicability is less dependent on interfacial phase formation and therefore be effective regardless of various surface finishes used in industry [17]. In addition, the extrinsic toughening of the solder is highly dependent on parameters such as low elastic modulus (to provide high compliance) and low yield strength (to provide high plastic energy dissipation ability). Thus, the present work investigates the effect of Al addition to the low Ag-content Sn–1Ag–0.5Cu solder on the bulk alloy microstructure and mechanical properties.

2 Experimental procedures

The Sn–1Ag–0.5Cu, Sn–1Ag–0.5Cu–0.1Al and Sn–1Ag–0.5Cu–0.2Al bulk solder specimens with a flat dog-bone shape were used in this study. Figure 1 shows the solder bar specimen and its dimensions. The thickness of the solder bar is 5 mm. The alloys were prepared by melting the Al with a pure Sn ingot in an induction furnace to make the master alloy (Sn + 2 wt. % Al). Next, the master alloy was sent to a third party lab (SGS) to confirm the Al element concentration. The Sn–Al, Sn–Ag and Sn–Cu master alloys were mixed with pure liquid Sn in a melting furnace for 60 min in an atmospheric environment at 290–300, 350–360 and 420–430 °C for the Sn–1Ag–0.5Cu, Sn–1Ag–0.5Cu–0.1Al and Sn–1Ag–0.5Cu–0.2Al solders, respectively. The chemical compositions were analyzed by Atomic Emission Spectrometry (AES) to ensure that Sn, Ag, Cu and the impurity of the alloy composition met the specifications (see Table 1). Then, the molten alloys were poured into pre-heated stainless steel molds, and the molds were naturally air-cooled to room temperature (25 °C).

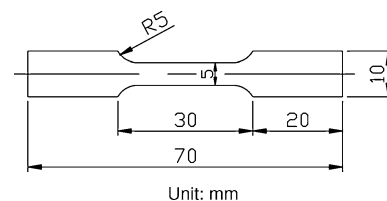


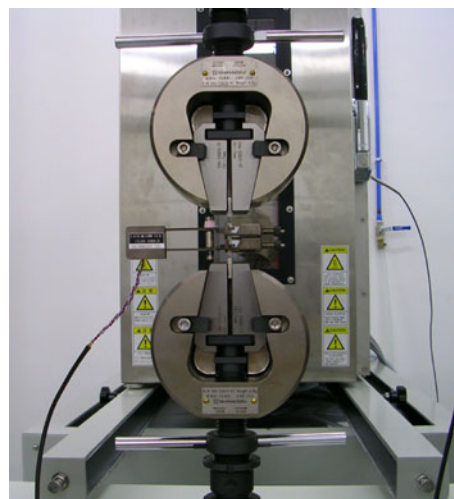
Fig. 1 Solder bar specimen

Table 1 Chemical composition of the alloys (wt. %)

Solder alloy	Sn	Ag	Cu	Fe	Pb	Sb	Al	As	Bi	Cd	Zn	In	Ni
SAC105	98.3815	1.0446	0.5070	0.0021	0.0067	0.0042	0.0005	<0.0001	0.0019	0.0001	0.0002	0.0019	0.0493
SAC105–0.1Al	98.3769	1.0098	0.5011	0.0011	0.0062	0.0044	0.0957	0.0001	0.0022	0.0001	0.0002	0.0023	–
SAC105–0.2Al	98.2124	1.0184	0.5398	0.0008	0.0061	0.0038	0.1946	0.0001	0.0017	0.0001	0.0001	0.0016	–

Finally, the molds were disassembled, and the dog-bone samples were removed and visually inspected to ensure that the surface of the parallel area was without damage and voids. The melting behavior of the solder alloys was investigated using differential scanning calorimetry (DSC). The sample alloy with a sample size of approximately 2.2 mg was used for DSC analysis. To obtain melting property data, the sample of SAC105 alloy was held for 1 min at 207 °C and was then heated from 207 °C to 236 °C with a scanning rate of 5 °C/min. The sample was subsequently cooled down from 207 °C to 65 °C at 100 °C/min, and then held for 15 min at 65 °C. The samples of SAC105–0.1Al and SAC105–0.2Al alloys were held for 1 min at 190 °C and were then heated from 190 °C to 240 °C and 260 °C, respectively with a scanning rate of 5 °C/min. The samples were subsequently cooled down to 65 °C at 100 °C/min, and then held for 15 min at 65 °C.

Before the tensile testing, the specimens were annealed at 100 °C for 2 h to decrease the residual stress induced during the sample preparation. Then, the solder bar was set onto a testing grip at two ends of the specimen using the Instron 5569A universal testing machine as shown in Fig. 2. An extensometer was then secured onto the specimen surface to measure the strain of the solder. In this study, 10 mm was used as a gauge length. Three different solders were prepared with the following nominal composition: Sn–1Ag–0.5Cu, Sn–1Ag–0.5Cu–0.1Al and Sn–1Ag–0.5Cu–0.2Al. Fifteen samples were tested under the same testing conditions for each solder specimen to obtain reliable and repeatable results. The test data were averaged to calculate the specimens' tensile properties. Tensile tests were carried out to investigate the effect of Al addition on the mechanical properties of Sn–1.0Ag–0.5Cu alloy such as elastic modulus, yield strength and ultimate tensile strength (UTS). Tensile tests were conducted at room temperature (25 °C) and at a constant strain rate of 10^{-3} s⁻¹. In this paper, the elastic modulus of solder was obtained from the elastic part of the tensile stress–strain curve. The yield strength of solder was considered as the stress value at which 0.2 % plastic strain occurs. The UTS of solder was considered as the maximum stress in the stress–strain curve. The microstructure, morphology and elemental analysis were carried out with conventional scanning electron microscopy (SEM), field emission SEM (FESEM) (zeiss ultra-60 FESEM) and energy dispersive X-ray spectroscopy (EDX) (EDAX-genesis utilities).

**Fig. 2** Tensile testing setup

Electron backscatter diffraction (EBSD) analysis was also carried out to determine the IMC phases. The SEM specimens were prepared through dicing, resin molding, grinding and polishing processes. The specimens were ground with four grades of SiC paper (#800, #1,200, #2,400 and #4,000), and then mechanically polished with a diamond suspension (3 μm). Finally, the specimens were polished with colloidal silica suspension (0.04 μm).

3 Results and discussion

3.1 Tensile properties of the alloys

The stress–strain curves of the standard SAC105 and Al-containing SAC105 solders are shown in Fig. 3. As illustrated, adding Al to the SAC105 alloy significantly affected mechanical properties. Figure 4 shows the mechanical properties of elastic modulus, 0.2 % proof stresses, ultimate tensile strengths (UTS) and total elongation for the SAC105, SAC105–0.1Al and SAC105–0.2Al solders. The addition of 0.1 wt. % Al reduces the elastic modulus, yield strength and UTS. On the other hand, the 0.2 wt. % Al addition brings the yield strength up to SAC105 level and the UTS up to level slightly higher than that of SAC105, while its effect on reducing the elastic modulus becomes less dependent compared with the 0.1 wt. % Al addition. Moreover, both 0.1 and 0.2 wt. % Al additions deteriorate the total elongation.

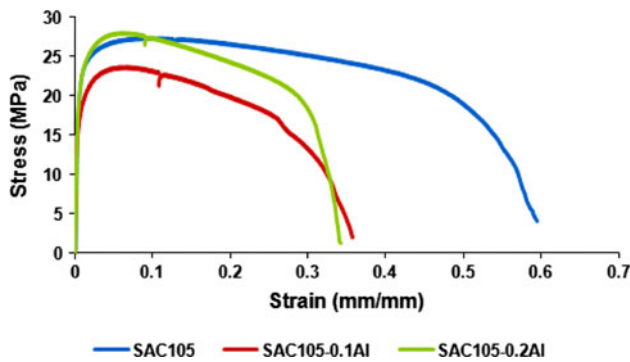


Fig. 3 Stress–strain curves for SAC105, SAC105–0.1Al and SAC105–0.2Al solders

As a solder joint material, the SAC105 solder alloy has been reported to have good drop impact reliability [26, 27]. This can be attributed to the low elastic modulus and yield strength and the large elongation of the SAC105 alloy, which result in a soft and highly compliant bulk solder joint. Thus, the SAC105 alloy can dissipate high dynamic energy through bulk solder deformation, which reduces the dynamic stress transferred to the interface IMC layers during drop impact loading conditions. Referring to Fig. 4a, b, the SAC105–0.1Al bulk solder has elastic modulus that is about 47 % lower than that of the SAC105 and yield strength that is about 19 % lower than that of the SAC105. That is, the 0.1 wt. % Al addition to the SAC105 bulk solder reduces the elastic modulus and yield strength. This reduction increases the bulk compliance and plastic energy dissipation ability, which are believed to play an important role in drop impact performance enhancement. The high elastic compliance and high plastic energy dissipation ability are key material properties to be optimized for extrinsic toughening [12–28]. The extrinsic toughening refers to a toughening mechanism attained by reducing the effective crack driving force that the crack tip actually experiences, through various energy dissipation processes without increasing inherent fracture resistance of the material or interface [29]. On the other hand, the SAC105–0.2Al bulk solder has elastic modulus that is about 21 % lower than that of the SAC105 (see Fig. 4a), while the yield strength is about the same as that of the SAC105 (see Fig. 4b). Thus, the addition of the 0.2 wt. % Al to the SAC105 solder is less effective in reducing the elastic modulus compared to the 0.1 wt. % Al addition. Moreover, the reduction in yield strength has been shown to stop with 0.2 wt. % Al addition. This observation implies that Al is a softening and strengthening element for the SAC105 solder alloy. It is worth to notice that the elongation of the Al added solders is lower than that of the SAC105 (see Fig. 4d). Thus, the SAC105 without Al has the ability to withstand much more plastic deformation than the two alloys with Al.

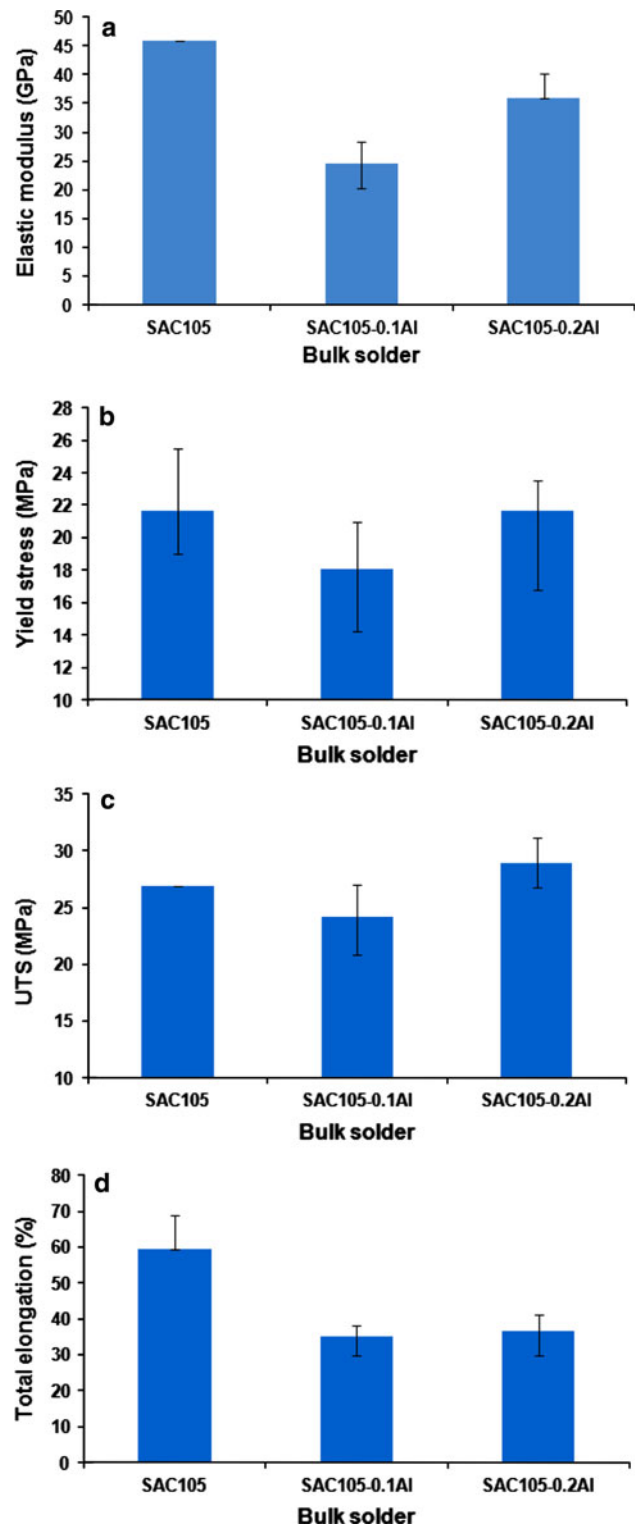


Fig. 4 Tensile properties for SAC105, SAC105–0.1Al and SAC105–0.2Al solders: **a** elastic modulus, **b** yield strength, **c** UTS and **d** total elongation

It is well known that the strain rate experienced by solders joint during drop impact testing is estimated to be $10^2/\text{sec}$, which belongs to dynamic-to-impact loading

condition. Under this condition, metallic materials are generally subject to a strain rate sensitivity phenomenon [12–28]. In this regime, metallic materials including solders become stronger or plastic deformation is more difficult with increasing strain rate. Since solders typically operate at very high homologous temperatures (~ 0.6) even

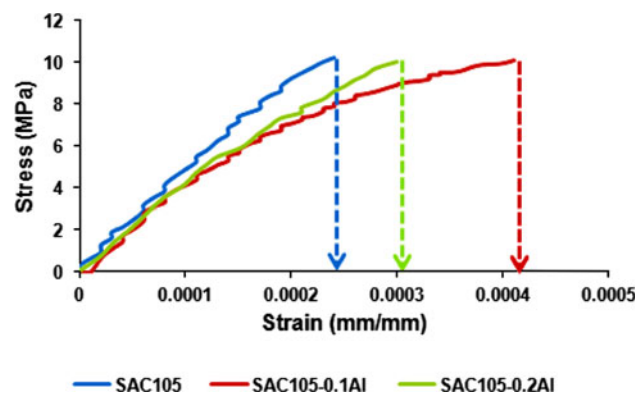


Fig. 5 The elastic portion of stress–strain curve for SAC105, SAC105–0.1Al and SAC105–0.2Al solders

at room temperature, considerable strain-rate sensitivity is exhibited by solders. Therefore, plastic deformation is suppressed under these high strain rates. Under this situation, the elastic compliance becomes a more significant material property in governing solder joint deformation and therefore stress transfer without global plastic deformation to the solder joint during drop test. That is, the performance of the bulk solder during drop impact loading conditions is dominated by elasticity. Figure 5 shows only the elastic portion of the stress–strain curve of the standard SAC105 and Al-containing SAC105 bulk solders. The SAC105–0.1Al and SAC105–0.2Al bulk solders have higher elastic compliance than the SAC105, and as a result, the stress on the SAC105–0.1Al and SAC105–0.2Al alloys is lower than that on the standard SAC105 alloy at the same strain. Thus, the SAC105–0.1Al and SAC105–0.2Al solders with a higher elastic compliance are expected to exhibit longer strain to failure than the standard SAC105 solder with lower elastic compliance. However, SAC105–0.2Al is less effective in increasing the elastic compliance than the SAC105–0.1Al. Moreover, too much Al addition over 0.1 wt. % results in a poor wetting property due to an increase in surface oxide [22].

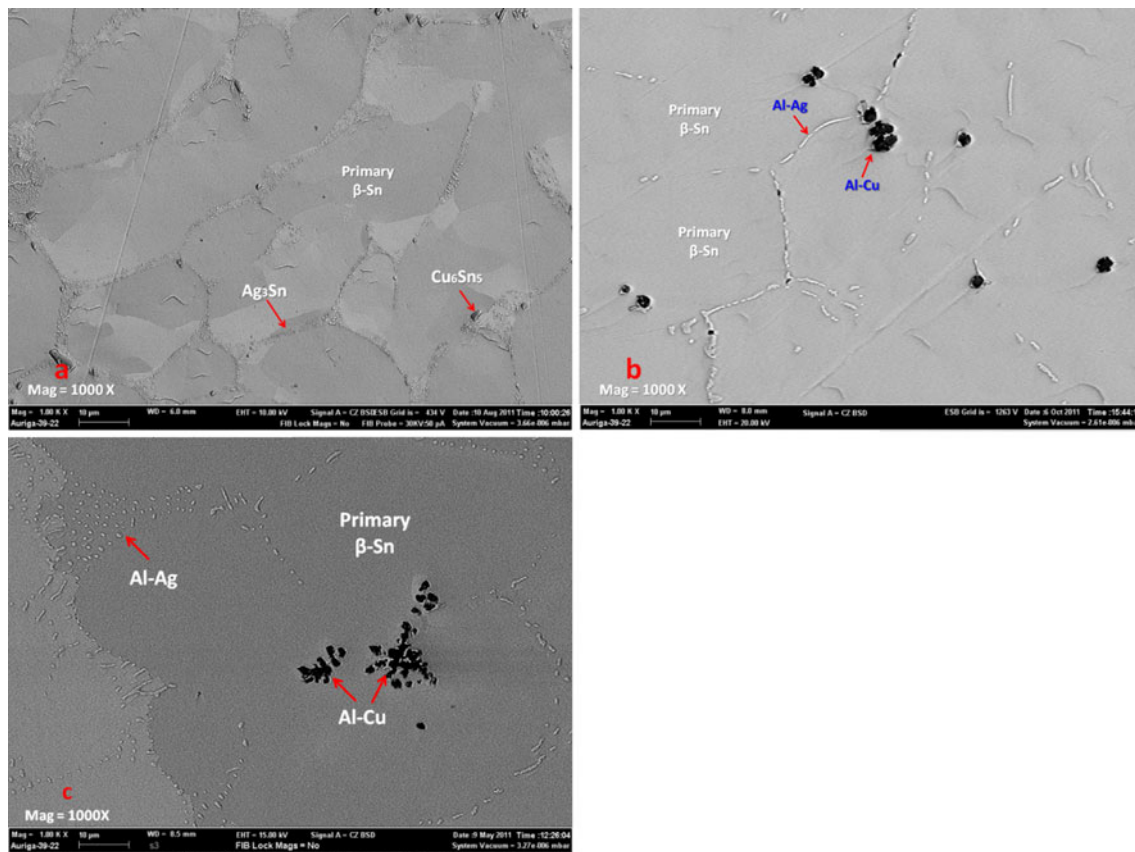


Fig. 6 SEM micrographs of **a** SAC105, **b** SAC105–0.1Al and **c** SAC105–0.2Al solders

3.2 Microstructures of the alloys

Figure 6a, b, c show the as-cast microstructures of the SAC105, SAC105–0.1Al and SAC105–0.2Al solders, respectively. Referring to Fig. 6a, the microstructure of the SAC105 solder consists of large primary β -Sn grains surrounded by eutectic regions of Ag_3Sn and Cu_6Sn_5 intermetallic compounds (IMC) dispersed within Sn-rich matrix. The microstructure of SAC105–0.1Al solder shown in Fig. 6b consists of large primary β -Sn grains surrounded by eutectic regions of three types of IMC particles dispersed in Sn-rich matrix. The magnified micrographs of the eutectic region are presented in Fig. 7a, b. The EDS analysis results have indicated that the large dark particles shown in Fig. 7a are $\text{Cu}_{69.63}\text{-Al}_{24.98}\text{-Sn}_{05.38}$ (see Fig. 8a); the large gray particles shown in Fig. 7a, b are $\text{Ag}_{65.44}\text{-Al}_{101.44}\text{-Sn}_{33.08}$ (see Fig. 8b); and the fine bright particles shown in Fig. 7b are $\text{Ag}_{27.33}\text{-Sn}_{72.67}$ (see Fig. 8c). SEM element mapping was also carried out, as shown in Fig. 9. The concentration of Ag, Cu and Al has a sudden rise at the location of the bulk IMC particles, while the concentration of Sn becomes small at the location of the bulk IMC particles. This indicates that the elements Ag, Cu and Al constitute the bulk IMC particles. Presumably the large dark and large gray particles are primarily IMC of Al–Cu and Al–Ag partially mixed with Sn, respectively. The fine bright particles are speculated to be Ag_3Sn IMC particles. The results of SAC105–0.2Al solder are in line with those observed in SAC105–0.1Al solder.

It is well known that, to a large extent, the microstructural characteristics of an alloy determine its mechanical performance. The Ag_3Sn and Cu_6Sn_5 phases have been reported to possess a much higher strength than the bulk material in the SAC alloys, whereas the primary β -Sn phase has the lowest elastic modulus and lowest yield strength among the bulk constituent phases in the SAC alloys [12, 27, 28]. Thus, the large amount of Ag_3Sn and

Cu_6Sn_5 phases increases the elastic modulus and yield strength, resulting in a stiff bulk solder. On the other hand, the presence of a high fraction of the primary β -Sn phase reduces the elastic modulus and yield strength, resulting in a soft and highly compliant bulk solder. Referring to Fig. 6a, the microstructure of the SAC105 alloy consists of relatively large primary β -Sn grains and small Ag_3Sn and Cu_6Sn_5 IMC particles sparsely distributed within the eutectic regions. Thus, the low elastic modulus and the low yield strength of the SAC105 solder can be attributed to the large primary β -Sn grains and the small amount of Ag_3Sn IMC particles.

Referring to Figs. 6b and 7, the microstructure of the SAC105 alloy containing 0.1 wt. % Al consists of large primary β -Sn grains and eutectic regions with large and sparsely distributed Al–Ag and Al–Cu IMC particles. Moreover, a small amount of Ag_3Sn IMC particles can be observed in the eutectic regions. Al has a great solubility in Cu, while the solid solubility of Cu in Al is restricted [30], and hence it is likely that Al and Cu form an Al-rich or Cu-rich phase that would transfer to the Al–Cu intermetallic compounds. Al has around 3 % solubility in Ag at 200 °C, [31] while Ag exhibits around 1 % solubility in Al. Al and Sn exhibit a eutectic temperature of 228.3 °C at 0.5 % Sn, [32] yet there is nearly zero solubility of each other at temperatures below 200 °C. On the basis of this information, it seems reasonable to say that the coexistence of Al with Ag and Cu is at least in correspondence with the anticipation that Al has solubility in Ag [31] and Cu [30] yet nearly zero solubility in Sn [32]. Thus, the 0.1 wt. % Al addition to the SAC105 bulk solder suppresses the formation of the Cu_6Sn_5 and forms larger Al–Cu IMC particles. Concurrently, the 0.1 wt. % Al addition significantly reduces the amount of the Ag_3Sn and forms larger Al–Ag IMC particles. It is well known that fine particles in alloys impede dislocation movement more efficiently, and produce an alloy with greater yield strength. When these

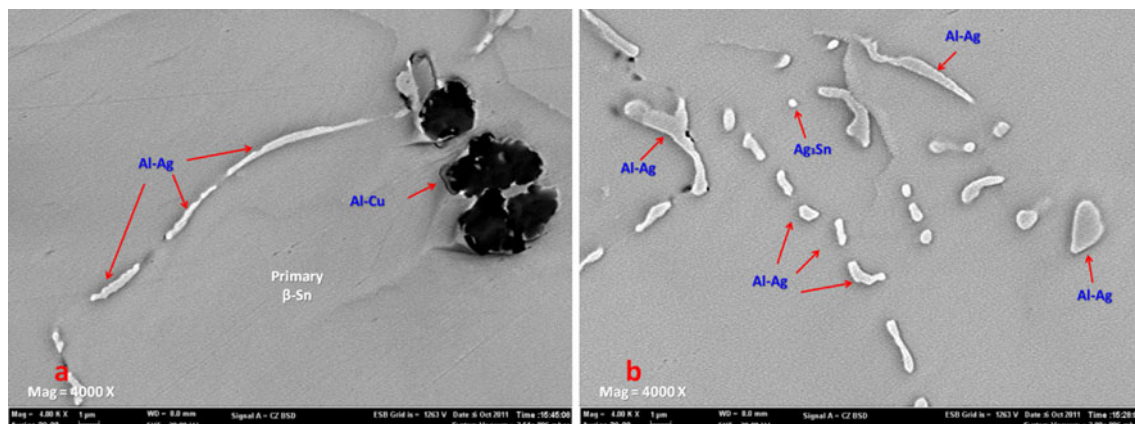


Fig. 7 SEM micrographs of eutectic region for SAC105–0.1Al solder

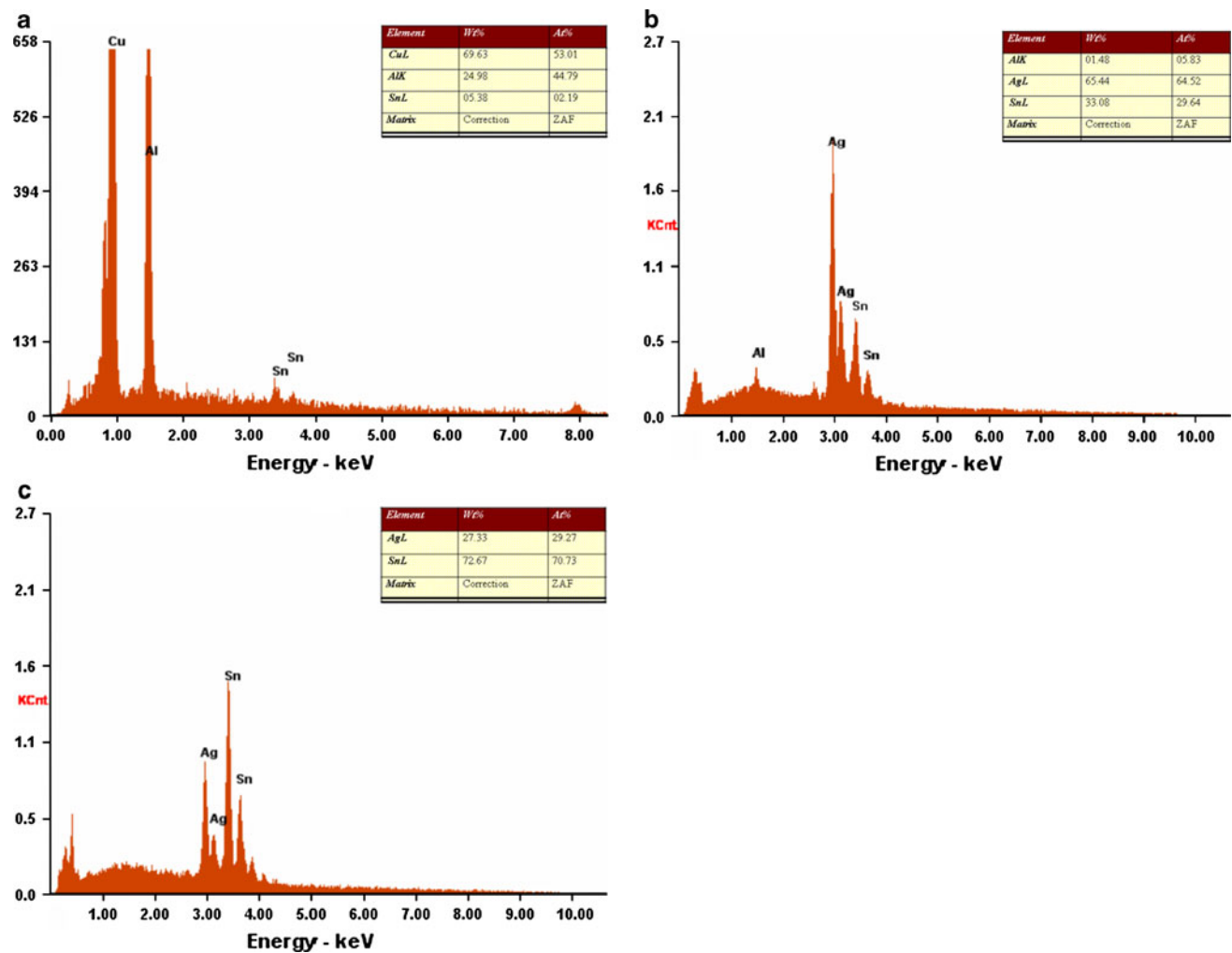


Fig. 8 EDS analysis result of the IMC particles in the SAC105–0.1Al solder

particles grow in size, the yield strength decreases. In addition, when the coherency of particles within the matrix is gradually lost when particles grow, the yield strength is further decreased [33]. In light of this mechanism, the small Ag_3Sn and Cu_6Sn_5 are replaced with larger Al–Ag and Al–Cu IMC particles, thereby resulting in a reduction of the elastic modulus and the yield strength. Summarily, the existence of larger Al–Ag and Al–Cu IMC particles in the eutectic regions surrounding the large primary β -Sn grains in the SAC105–0.1Al solder reduces the elastic modulus and yield strength.

However, as Al concentration increases from 0.1 to 0.2 wt. %, the reduction in the elastic modulus and yield strength becomes less significant. This can be attributed to increase the amount of Al–Ag IMC particles with increasing Al, which leads to reduce the spacing between these particles (see Fig. 6b, c), thus retarding the dislocation movement [34]. Moreover, as Al concentration increases from 0.1 to 0.2 wt. %, the particles size of Al–Ag

decreases (see Fig. 6b, c). However, the size of these Al–Ag particles is still quite larger than the Ag_3Sn . To further study the effect of Al addition to the SAC105 bulk solder. The fracture surfaces were examined after tensile tests. Figure 10 shows SEM micrographs of the fracture surfaces of Sn–1Ag–0.5Cu–xAl alloys ($X = 0, 0.1$ and 0.3 wt. %). All alloys displayed a ductile fracture mode. The dimpled pattern is represented in all fracture surfaces. The fracture surface of the SAC105 solder consists of large ductile-dimples (see Fig. 10a). These results demonstrate the fracture mechanism is microvoid coalescence fracture. For the SAC105–0.1Al and SAC105–0.2Al solders, the fracture surface with the elongated dimples along a trace of shear stress (see Fig. 10b, c) is indicative of a ductile shear fracture. The reduction of tensile strength and elongation for the Al added solders may be related to the weak interface between the large Al–Ag and Al–Cu IMCs with the β -Sn matrix. Thus, rather than ductile cup-cone, ductile shear fracture surface is exposed after tensile test.

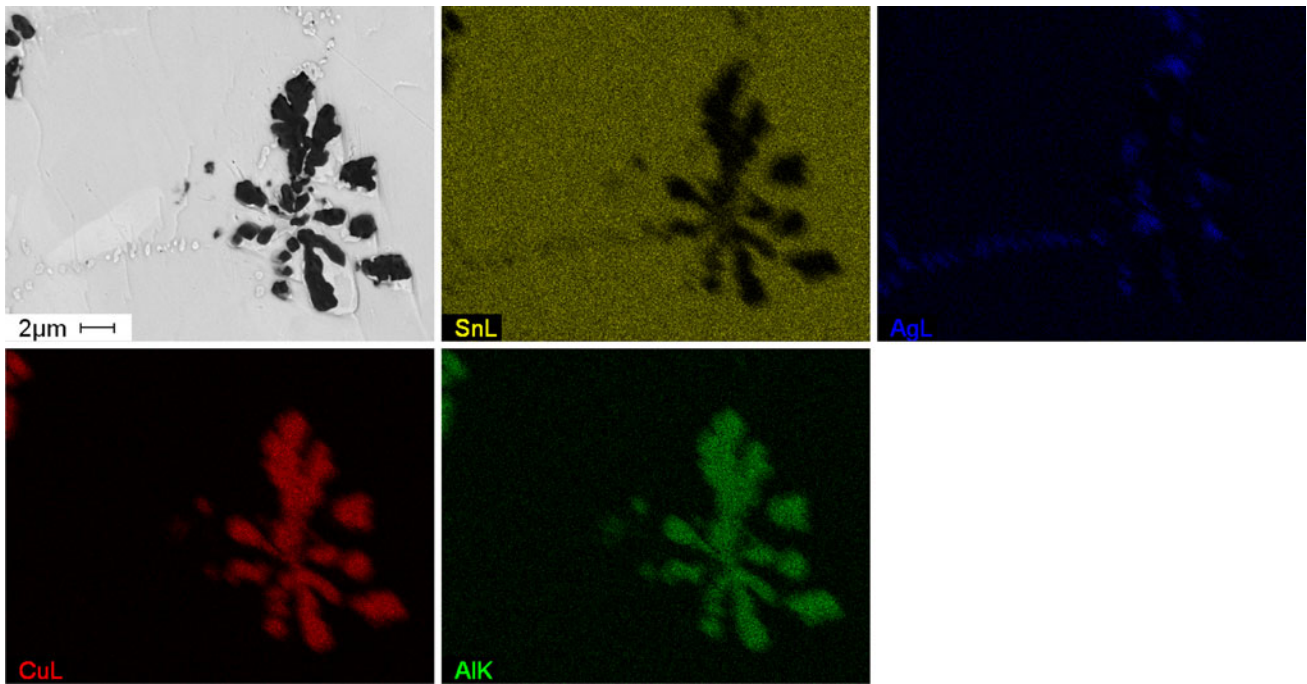


Fig. 9 SEM element mapping of SAC105–0.1Al solder

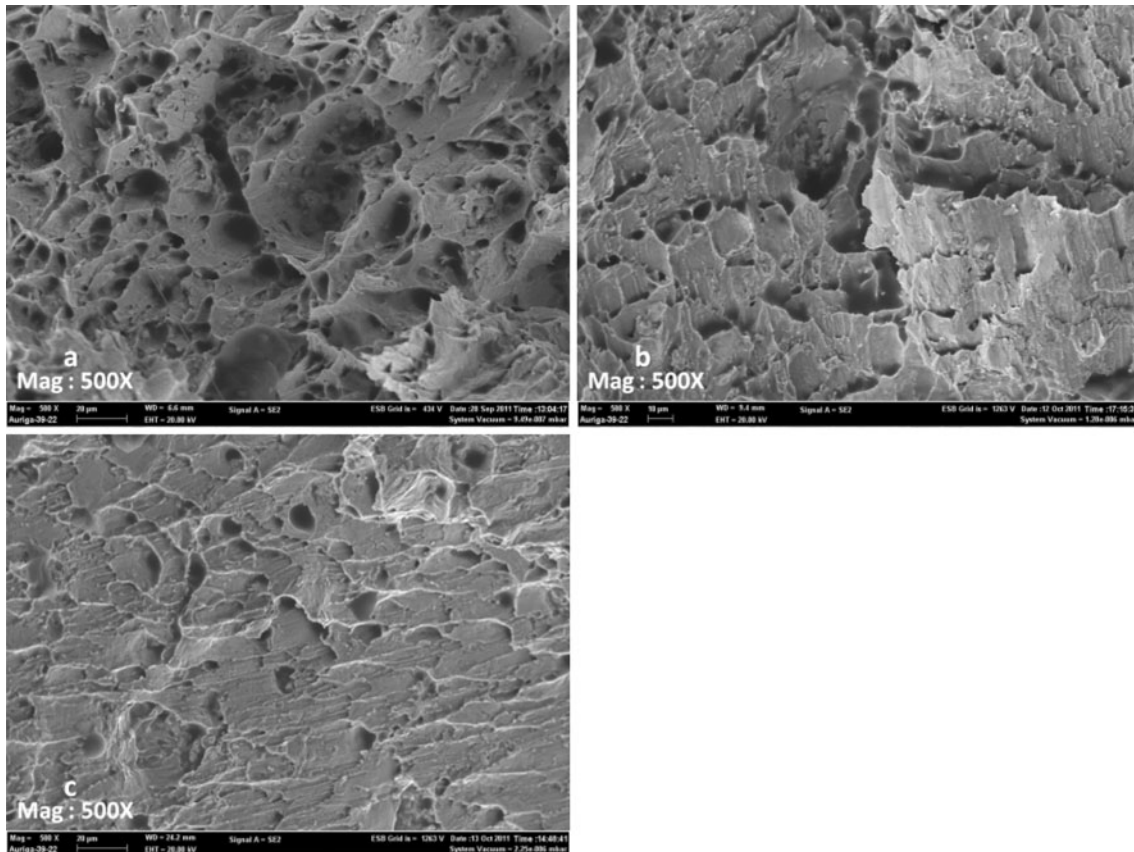


Fig. 10 SEM fractographs of the alloys after tensile tests: **a** SAC105, **b** SAC105–0.1Al and **c** SAC105–0.2Al

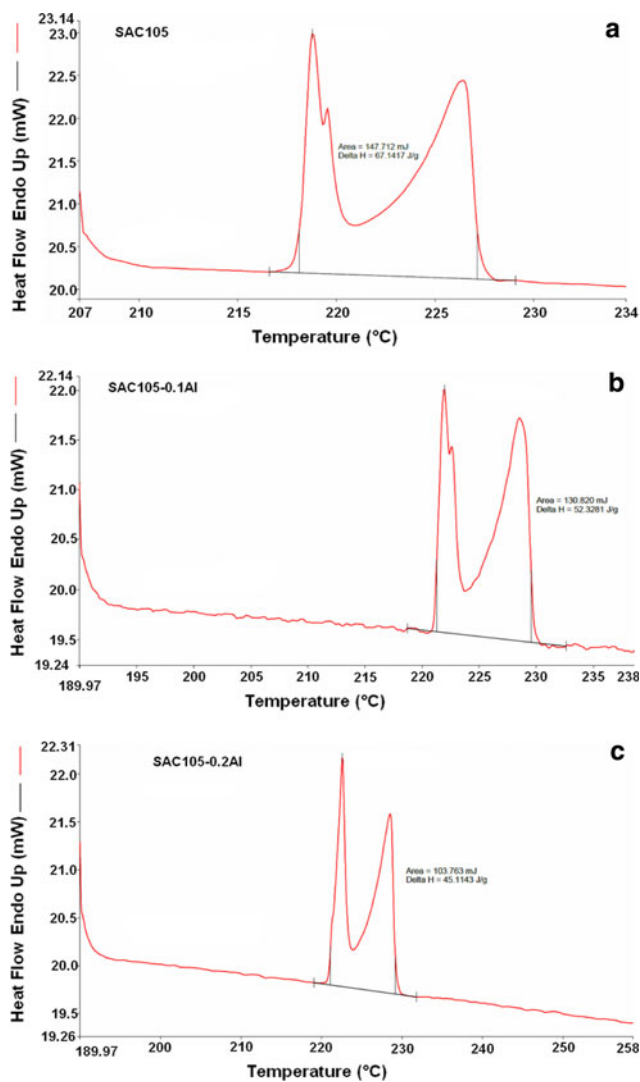


Fig. 11 DSC thermographs of **a** SAC105, **b** SAC105–0.1Al and **c** SAC105–0.2Al solders

Table 2 Differential scanning calorimetry (DSC) test results of the alloys

Alloys	Solidus (°C)	Liquidus (°C)	Pasty range
SAC105	218.11	227.16	9.05
SAC105–0.1Al	221.33	229.58	8.25
SAC105–0.2Al	221.09	229.04	7.95

3.3 Thermal behavior

DSC analysis was carried out to determine the effects of the Al addition on the melting temperature/range of the standard SAC105 alloy. Figure 11 shows the DSC heating curves of the standard SAC105 and Al-containing SAC105 alloys. As can be seen from Fig. 11a, the SAC105 exhibit two endothermic peaks. Referring to Fig. 11b, c, the SAC105–0.1Al

and the SAC105–0.2Al alloys show two endothermic peaks similar to those of the SAC105 alloy. Compared with SAC105, Al-containing SAC105 alloys exhibit slightly higher solidus and liquidus temperatures, while slightly narrower pasty range (see Table 2). Increasing the Al content leads to slightly decrease the solidus and liquidus temperatures. Moreover, the pasty range slightly decreases from 8.25 °C to 7.95 °C due to increasing the Al content.

4 Conclusion

1. The 0.1 and 0.2 wt. % Al additions to the SAC105 bulk solder suppress the formation of Cu_6Sn_5 IMC particles and significantly reduce the number of Ag_3Sn IMC particles, and form larger Al–Cu and Al–Ag IMC particles.
2. The 0.1 wt. % Al addition to the SAC105 bulk solder further reduces the elastic modulus, yield strength and UTS. Increasing the Al concentration from 0.1 to 0.2 wt. %, brings the yield strength up to the level of SAC105 and the UTS up to level slightly higher than the SAC105, whilst its effect on reduction of elastic modulus becomes less dependent on increasing Al concentration.
3. The 0.1 and 0.2 wt. % Al additions to the SAC105 alloy deteriorate the total elongation.
4. The additions of 0.1 and 0.2 wt. % Al slightly increase both solidus and liquids temperatures of the SAC105 solder, and slightly reduce the pasty range, hence allowing the use of the Al-containing Sn–1Ag–0.5Cu alloys, to be consistent with the conditions of usage for conventional Sn–Ag–Cu solder alloys.

Acknowledgments The authors would like to acknowledge the financial support provided by University of Malaya (UM) under the IPPP Fund Project No.: PS117/2010B and the UMRG Fund under project No.: RG066/09AET.

References

1. M. Abteu, G. Selvaduray, Lead-free solders in microelectronics. *Mater. Sci. Eng., R* **27**, 95–141 (2000)
2. K.J. Puttlitz, G.T. Galyon, Impact of the ROHS directive on high-performance electronic systems. *J. Mater. Sci. Mater. Electron.* **18**, 347–365 (2007)
3. D.R. Frear, Issues related to the implementation of Pb-free electronic solders in consumer electronics. *J. Mater. Sci. Mater. Electron.* **18**, 319–330 (2007)
4. R. Plieninger, M. Dittes, K. Pressel, Modern IC packaging trends and their reliability implications. *Microelectron. Reliab.* **46**, 868–1873 (2006)
5. R.S. Pandher, B.G. Lewis, R. Vangaveti, B. Singh, Drop shock reliability of lead-free alloys—effect of micro-additives, in *Proceedings of 57th IEEE-ECTC Conference*, 2007, pp. 669–676
6. D.A. Shnawah, M.F.M. Sabri, I.A. Badruddin, A review on thermal cycling and drop impact reliability of SAC solder joint in

- portable electronic products. *Microelectron. Reliab.* **52**, 90–99 (2012)
7. B. Huang, H.-S. Hwang, N.-C. Lee, A compliant and creep resistant SAC–Al (Ni) alloy, in *Proceedings of 9th IEEE-EPTC Conference*, 2007, pp. 693–701
 8. D.Y.R. Chong, F.X. Che, J.H.L. Pang, K. Ng, J.Y.N. Tan, P.T.H. Low, Drop impact reliability testing for lead-free and lead-based soldered IC packages. *Microelectron. Reliab.* **46**, 1160–1171 (2006)
 9. E.H. Wong, S.K.W. Seah, V.P.W. Shim, A review of board level solder joints for mobile applications. *Microelectron. Reliab.* **48**, 1747–1758 (2008)
 10. E.H. Wong, S.K.W. Seah, W.D.V. Driel, J.F.J.M. Caers, N. Owens, Y.-S. Lai, Advances in the drop-impact reliability of solder joints for mobile applications. *Microelectron. Reliab.* **49**, 139–149 (2009)
 11. B. Zhang, H. Ding, X. Sheng, Reliability study of board-level lead-free interconnections under sequential thermal cycling and drop impact. *Microelectron. Reliab.* **49**, 530–536 (2009)
 12. D. Kim, D. Suh, T. Millard, H. Kim, C. Kumar, M. Zhu, et al., Evaluation of high compliant low Ag solder alloys on OSP as a drop solution for the 2 level Pb-free interconnection, in *Proceedings of 57th IEEE-ECTC Conference*, 2007, pp. 1614–1619
 13. R.S. Pandher, B.G. Lewis, R. Vangaveti, B. Singh, Drop shock reliability of lead-free alloys—effect of micro-additives, in *Proceedings of 57th IEEE-ECTC*, 2007, pp. 669–676
 14. F.X. Che, W.H. Zhu, E.S.W. Poh, X.W. Zhang, X.R. Zhang, The study of mechanical properties of Sn–Ag–Cu lead-free solders with different Ag contents and Ni doping under different strain rates and temperatures. *J. Alloy. Compd.* **507**, 215–224 (2010)
 15. A.M. Yu, J.W. Jang, J.K. Kim, J.H. Lee, M.S. Kim, Improved reliability of Sn–Ag–Cu–In solder alloy by the addition of minor elements, in *Proceedings of 60th IEEE-ECTC Conference*, 2010, pp. 1524–1528
 16. W. Kittidacha, A. Kanjanavikat, K. Vattananiyom, Effect of SAC alloy composition on drop and temp cycle reliability of BGA with NiAu pad finish, in *Proceedings of 10th IEEE-EPTC Conference*, 2008, pp. 1074–1079
 17. Y. Kariya, T. Hossi, S. Terashima, M. Tanaka, M. Otsuka, Effect of silver content on the shear fatigue properties of Sn–Ag–Cu flip-chip interconnect. *J. Electron. Mater.* **33**, 321–328 (2004)
 18. M. Tanaka, T. Sasaki, T. Kobayashi, K. Tatsumi, Improvement in drop shock reliability of Sn–1.2Ag–0.5Cu BGA interconnects by Ni addition, in *Proceedings of 56th IEEE-ECTC Conference*, 2006, pp. 78–84
 19. R. Pandher, R. Healey, Reliability of Pb-free solder alloys in demanding BGA and CSP applications, in *Proceedings of 58th IEEE-ECTC Conference*, 2008, pp. 2018–2023
 20. W. Liu W, N.-C. Lee, A. Porras, Ding M, Gallagher A. Achieving high reliability low cost lead-free SAC slider joints via Mn or Ce doping, in *Proceedings of 59th IEEE-ECTC Conference*, 2009, pp. 994–1007
 21. A.-M. Yu, J.-K. Kim, J.-H. Lee, M.-S. Kim, Tensile properties and drop/shock reliability of Sn–Ag–Cu–In based solder alloys, in *Proceedings of 11th IEEE-EPTC Conference*, 2009, pp. 679–682
 22. Y.W. Lee, I.H. Kim, E.S. Kim, J.H. Lee, J.T. Moon, Improvement of wettability and drop impact reliability by Al addition in SnAgCu Solder, in *Proceedings of 12th IEEE-EPTC Conference*, 2010, pp. 429–432
 23. A.K. Gain, T. Fouzder, Y.C. Chan, A. Sharif, N.B. Wong, W.K.C. Yung, The influence of addition of Al nano-particles on the microstructure and shear strength of eutectic Sn–Ag–Cu solder on Au/Ni metallized Cu pads. *J. Alloy. Compd.* **506**, 216–223 (2010)
 24. Y.K. Jee, Y.-H. Xia, J. Yu, H.-W. Kang, and T.-Y. Lee, in *Proceedings of 58th IEEE-ECTC Conference*, 2008, pp. 491–494
 25. H.R. Kotadia, O. Mokhtari, M. Bottrill, M.P. Clode, M.A. Green, S.H. Mannan, Reactions of Sn–3.5Ag-based solders containing Zn and Al additions on Cu and Ni(P) substrates. *J. Electron. Mater.* **12**, 2720–2731 (2010)
 26. A. Syed, J. Scanlan, S. Cha, W. Kang, E. Sohn, T. Kim, et al., Impact of package design and materials on reliability for temperature cycling, bend, and drop loading conditions, in *Proceedings of 58th IEEE-ECTC Conference*, 2008, pp. 1453–61
 27. W. Kittidacha, A. Kanjanavikat, K. Vattananiyom, Effect of SAC alloy composition on drop and temp cycle reliability of BGA with NiAu pad finish, in *Proceedings of 10th IEEE-ECTC Conference*, 2008, pp. 1074–1079
 28. D. Suh, D.W. Kim, P. Liu, H. Kim, J.A. Weninger, C.M. Kumar, A. Prasad, B.W. Grimsley, H.B. Tejada, Effects of Ag content on fracture resistance of Sn–Ag–Cu lead-free solders under high strain rate conditions. *Mater. Sci. Eng. A* **46–461**, 595–603 (2007)
 29. R.O. Ritchie, Mechanisms of fatigue crack propagation in metals, ceramics and composites: role of crack tip shielding. *Mater. Sci. Eng. A* **103**, 15–28 (1988)
 30. M. Hanson, K. Anderko, *Constitution of Binary Alloys*, 2nd edn. (McGraw-Hill, New York, 1985), p. 84
 31. M. Hanson, K. Anderko, *Constitution of Binary Alloys*, 2nd edn. (McGraw-Hill, New York, 1985), p. 1
 32. M. Hanson, K. Anderko, *Constitution of Binary Alloys*, 2nd edn. (McGraw-Hill, New York, 1985), p. 135
 33. G. E Dieter, *Mechanical Metallurgy*, 2nd edn. (McGraw-Hill, Tokyo, 1976), p. 222
 34. G. E Dieter, *Mechanical Metallurgy*, 2nd edn. (McGraw-Hill, Tokyo, 1976), p. 224